Lidar observations of the vertical distribution of stratospheric ozone over Tomsk in summer 1998

V.N. Marichev, V.V. Zuev, P.A. Khryapov, S.I. Dolgii, and A.V. Nevzorov

Institute of Atmospheric Optics,
Siberian Branch of the Russian Academy of Sciences, Tomsk
Received December 28, 1998

Lidar observations of the vertical ozone distribution in the atmosphere over Tomsk are analyzed. The observations were conducted in summer 1998. The lidar setup is described. Lidar return signals were corrected for miscounts due to pile up of single-electron pulses at signal recording in the photon-counting mode. The ozone profile was averaged over the three summer months. This profile is indicative of the ozone deficit of 20–25 % in the area of maximum ozone layer as compared with the Krueger model. The highest variability of the ozone content has been noticed in the lower part of the layer at altitudes of 15 to 16 km. As the altitude further increases, the variability decreases monotonically. Data obtained in lidar measurements were used for calculation of the ozone column in the 15–30 km layer. Comparing time series of data on the ozone column measured with l −124 ozonometer and the integral column ozone, we have found the correlation coefficient $K = 0.47$. The ozone percentage in the 15–30 km layer has been found to be (61.6 ± 5.6) %. The vertical profile of the coefficient of correlation between the ozone concentration and temperature has been drawn. The correlation proved to be positive in the 16–26 and 28–32 km altitude ranges. The altitude ranges of 15 to 16 and 27 to 28 km are characterized by negative correlation. It is remarkable that secondary ozone maxima may arise just in these altitude ranges. These maxima are most likely related to the horizontal advection of polar air masses and the meridional circulation of the stratosphere.

1. Introduction

Detection of climate changes requires continuous monitoring of the ozone in the stratosphere, where it is primarily concentrated.[1] Discovery of the ozone holes over the Antarctic, Europe, and Siberia caused the need for global monitoring of ozone. The lidar method of observation over ozone is very important in this aspect. It supplements traditional ground-based methods (employing, for example, Dobson, Umkher, and Brewer foreign spectrophotometers or l −124 Russian spectrophotometer) and satellite ones (TOMS, SACE-II).

In 1977 Megie et al. (France) demonstrated for the first time the applicability of lidar to spatially resolved measurements of the atmospheric ozone. [2] They used a dye laser as a transmitter of radiation. In 1978 Uchino et al. (Japan) applied a more promising XeCl excimer laser to lidar sounding of ozone.[3] This laser is widely used in the up-to-date stratospheric lidars. Stratospheric ozone observations are currently conducted at a number of lidar stations situated mostly in the Northern Hemisphere.[4]

Lidar observations of the stratospheric ozone layer over Tomsk have been conducted since December 1988. Most profiles of the stratospheric ozone have been obtained in the winter–spring period. The profiles obtained for summer and fall seasons are few in number because of fewer number of clear-sky nights and high air humidity, which causes instrumental malfunctioning.

At the same time, the summer period is most interesting for studying the behavior of the stratospheric ozone layer because of a particularly low ozone content observed over West Siberia in this period. The summer deficit of ozone may have ecological and climate consequences. Study of vertical ozone distribution (VOD) in the stratosphere, especially in the area of localization of the ozone layer, and monitoring of the seasonal variability of the ozone column allow one to gain new knowledge about the mechanisms of transformation of the ozonosphere and its influence on the global climate.

2. Instrumentation: brief description of the lidar and correction of lidar returns

Block diagram of the modified UV lidar is shown in Fig. 1. The principal units of the lidar are the high-power XeCl excimer laser (pulse energy of 60 to 80 mJ, pulse repetition rate of 50 Hz) and the primary and auxiliary telescopes with the corresponding devices for spectral selection and data acquisition. The XeCl laser giving, after frequency conversion in a hydrogen SRS cell, the radiation at $\lambda_{on} = 308$ and $\lambda_{off} = 353$ nm in combination with the receiving system on the basis of Newtonian telescope forms the channel for sounding of stratospheric ozone. The use of small (Cassegrainian) telescope with the receiving mirror 0.25 m in diameter allows us to widen the dynamic range of lidar signals in the near zone and thus to create the tropospheric channel for ozone sounding. The well-known differential absorption method was used for obtaining and processing experimental data.
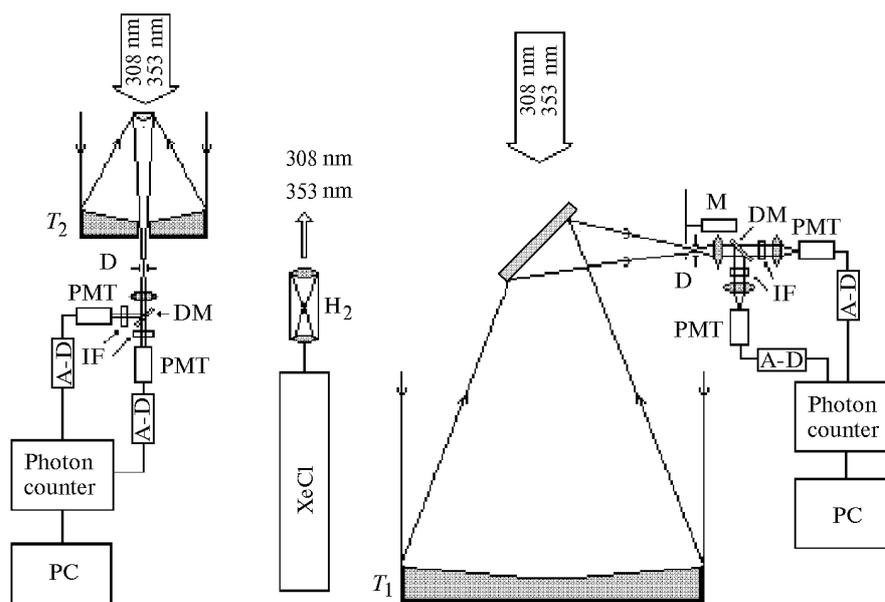
Fig. 1. Block diagram of the modified UV lidar: XeCl excimer laser (λ = 308 nm); H_2 SRS cell (m_2); large and small receiving telescopes (T_1 and T_2); field stop diaphragm (D); mechanical chopper (M); FEU-130 photomultiplier tube (PMT); interference filter (IF); dichroic mirror (DM); amplifier–discriminator (A-D); personal computer (pC).

Usually the altitude range of the vertical ozone distribution measurements is 13 to 35 km. It can be expanded to 5 to 50 km by suppressing return signals (i.e. by decreasing the photodetector overloading) from the near zone and increasing the altitude of sounding due to longer time of return signal accumulation. To obtain the statistically confident ozone profile up to altitudes of 30 to 35 km, the measurement time of ≈ 25 min is required at a spatial averaging over a range gate from 0.1 to 0.4 km.

Data of ozone sounding have been processed with the specially developed SOUND software package. The latest version of this software includes the program packages for calculation of temperature and scattering ratio.[6] The new and important advantage of this software is its capability of calculating with the allowance for aerosol stratification (through the scattering ratio) and temperature.

As mentioned above, when high-power lidar transmitter is used, a problem arises on recording intense lidar returns coming from the near zone. For the main receiving telescope with regard for mechanical chopping of lidar returns coming from lower altitudes, the near zone extends to the altitudes of 10 to 20 km. Reception of optical signals from such altitudes in the photon counting mode leads to underestimation of the measured power due to finite dead time of the recording system. Such a system necessarily includes an amplifier–generator and a counter of single-electron pulses (SPs) at the PMT output. The former generates a standard pulse at the threshold level of SP discrimination. The pulse comes to the counter. At high intensity of backscattered radiation, the SP count rate increases, and the probability of miscounts due to pulse pile up increases as well. In such a case, a PMT with a

recording channel is considered as a counter with the dead time of prolonged type.[7] The value of the dead time τ is determined by the SP width at the discrimination threshold level.

In commonly accepted Poisson statistics of photoelectrons, the pile up factor is taken into account through the relation[8]:

$$M = N \exp\left(-N\tau/n\Delta T\right),$$

where N and M are the numbers of incoming and recorded SPs; n is the number of measurements; ΔT is the time gate duration. This is the equation for true number of single-electron pulses N. It can be solved using the iteration technique under the initial condition that $N_0 = M$.

Figure 2a gives an example of recorded and corrected lidar return signals for a given SP width τ = 13 ns. As seen, signals at both wavelength of 308 and 353 nm are most distorted at the altitude of their maximum. Since the data from the altitude of 10 km were processed, the influence of signal correction extends for the altitude range of 10 to 20 km. Figure 2b demonstrates the initial ozone profile and that corrected for signal distortion. As expected, the profiles differ most markedly in the lower part, and the difference reaches 30 % in this case.

It should be noted that the performed analysis of data for signal correction at reconstruction of ozone profiles has shown the following. Correction is most efficient when only one of the return signals is highly intense. In the case, when both signals have high intensity, the distorting factor decreases due to compensating influence of data processing by the differential absorption method. The intensity of lidar

signals was estimated by the number of SPs in a single time gate, as well as by the ratio of the total time of the gate filling with incoming SPs to the time gate duration $K_N = N\tau/\Delta T$. For the recorded signals, the value of the coefficient K_N reached 0.18. According to Ref. 7, this value is below the critical level of 0.2 to 0.3. Thus, it is possible to correct the entire data array.
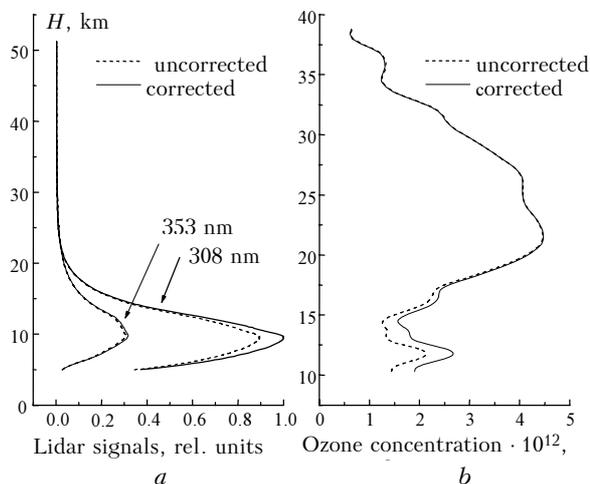

Fig. 2. Lidar return signals at the wavelengths λ_{on} and λ_{off} (*a*) and the ozone profiles reconstructed from them (*b*).

3. Lidar measurements of VOD in the stratosphere and their analysis

In June–August of 1998 26 night measurement sessions have been successfully carried out. Correspondingly, 26 averaged night profiles of VOD have been obtained. As a rule, the averaged ozone profile was reconstructed from three to four series of return signal accumulation (every was 25 minutes long). Reconstruction of individual VOD profiles for each series was possible as well. Figure 3 shows the individual vertical ozone profiles obtained on August 10, 1998, in three sounding series (*1, 2, 3*) and the profile obtained from the sum signal of all the three series (*4*).

Thus, starting from the altitude of 17 km, the three individual profiles behave similarly with altitude or even identically within the standard error σ. At the same time, at altitudes below 17 km the discrepancy between the profiles exceeds the error σ, and behavior of the latter is indicative of the ozone concentration dynamics. At the level of $m = 15$ km the values of ozone concentration deceased sequentially from one measurement series to another as $(2; 1.5; 1) \times 10^{12}$ mol/cm^3. In ozonometry it is known (and shown below in this paper) that the ozone column density varies most widely just at altitudes below the ozone peak. This variability is caused by the influence of dynamic processes. In this case, the presented example of night ozone sounding demonstrates reliability and stability of lidar measurements of ozone, as well as the possibility of observing the VOD dynamics.
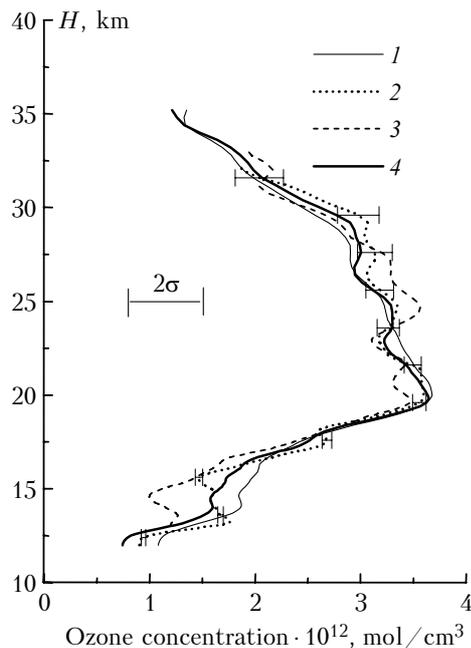

Fig. 3. Vertical ozone profiles obtained in the three consecutive sounding series and that obtained from the sum of all the three night series on August 10, 1998.

As was mentioned above, it of greatest interest for us was the construction of a summer mean ozone profile. Earlier it was impossible because of only a few number of corresponding data available. Figure 4 shows the night VOD profile and its variability along with the standard errors of calculation. The VOD profile presented has been averaged over three summer months. For comparison, Fig. 4 also shows the Krueger ozone model[9] and the winter–spring mean ozone profile obtained by us with the use of the lidar in 1995–1997 (Ref. 10). The entire lower part of the summer ozone profile up to the altitude of 27 km is characterized by the ozone deficit as compared to the model profile. The deficit is especially pronounced in the area of maximum ozone layer, where it reaches the values about 20–25 % in the altitude range from 15 to 25 km. As compared to winter–spring profiles, the ozone concentration in the summer profile is also markedly lower. This is rather typical of the seasonal stratification of ozone in the stratosphere of mid-latitudes.[1] As expected, the influence of the dynamic factor manifests itself in the highest VOD variability at lower altitudes. The increase of up to 100% is clearly seen at altitudes of 12 to 16 km. Then the curve decreases monotonically up to the altitude of 37 km with a slight local maximum near $m = 30$–32 km.

The mean ozone column density in atmospheric layers each 2 km thick for the same summer period is shown in Fig. 5 along with the variability and percentage of every layer with respect to the entire layer of 14 to 32 km. Similarly to the mean profile, the ozone column density varies most widely in the lower layer of 14 to 16 km, then a smooth decrease of σ is observed up to the altitude $m = 30$ km followed by some growth at 30–32 km.
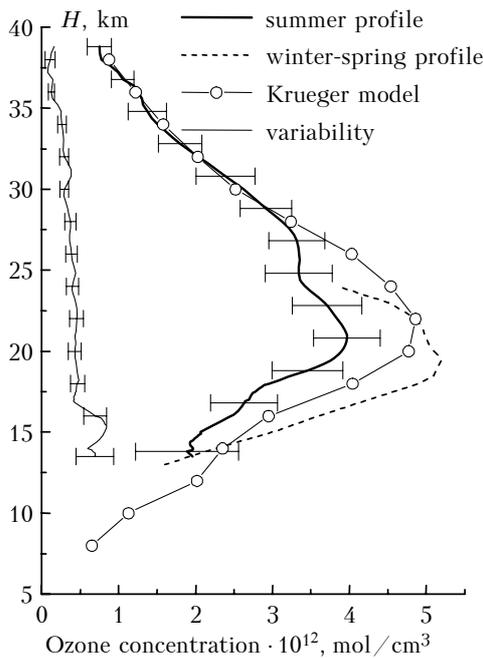
Fig. 4. Summer mean ozone profile for June–August 1998 in comparison with the Krueger model and the winter–spring mean ozone profile for 1995–1997.
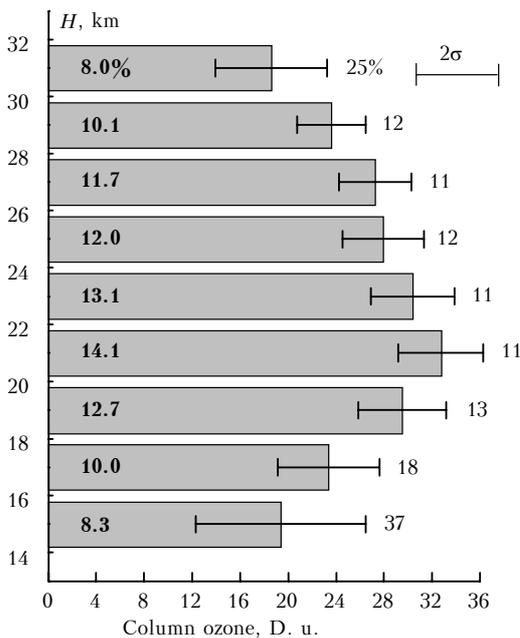

Fig. 5. Column ozone in different atmospheric layers.

Time behavior of the column ozone in the atmospheric layers is shown in Fig. 6. There is no somewhat marked correlation between the column ozone in different layers. Only two cases of a slight decrease in the ozone in the layers of 14–26 km and the ozone increase (decreasing with altitude) in the layers of 16 to 22 km can be noticed. In Fig. 6 the first case is marked by a downward arrow, while the second one is marked with an upward arrow.
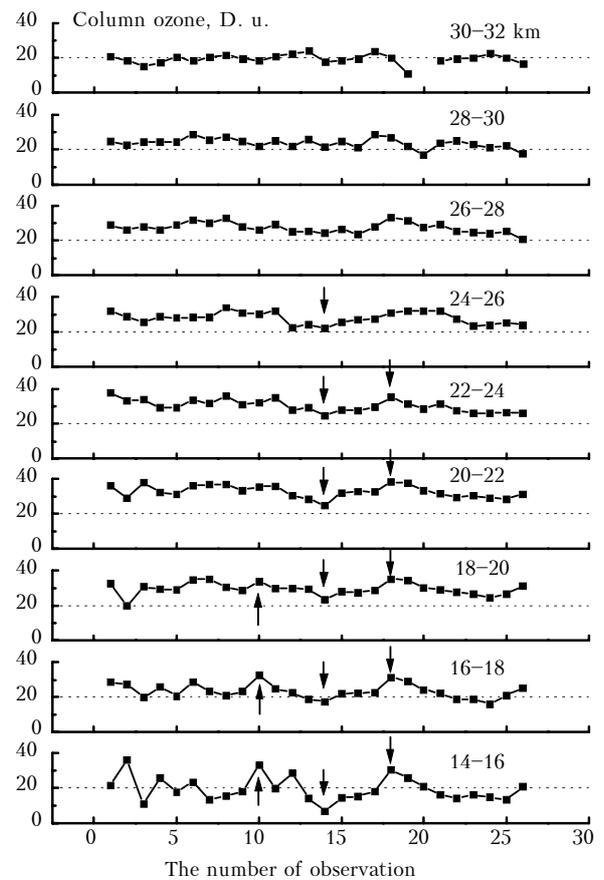

Fig. 6. Time behavior of ozone variability in 2-km thick atmospheric layers in summer 1998.

In the summer period under consideration, the total ozone content (TOC) in the atmosphere was routinely measured with an l −124 ozonometer. Since the series of measured values is practically continuous, we had an opportunity to select the data corresponding to the lidar measurements for their comparison. Since the l −124 device measured ozone concentration only in daytime, we took for our comparison the average of the ozonometer data obtained a day before and after the lidar measurements.

Figure 7 presents the series of and integral column ozone obtained from the lidar profile by integration over the layer of 15 to 30 km. As seen, the values correlate, and there is some tendency to a decrease in the column ozone. The calculated correlation coefficient K is 0.47, what is somewhat lower than the correlation coefficient $K = 0.73$, which has been found from a comparison between the lidar data and the data of spectrophotometer for May 1995 – April 1996 (Refs. 10 and 11). This peculiarity may be caused by stronger influence of the dynamic factor in the troposphere in summer period on the formation of the ozonosphere.
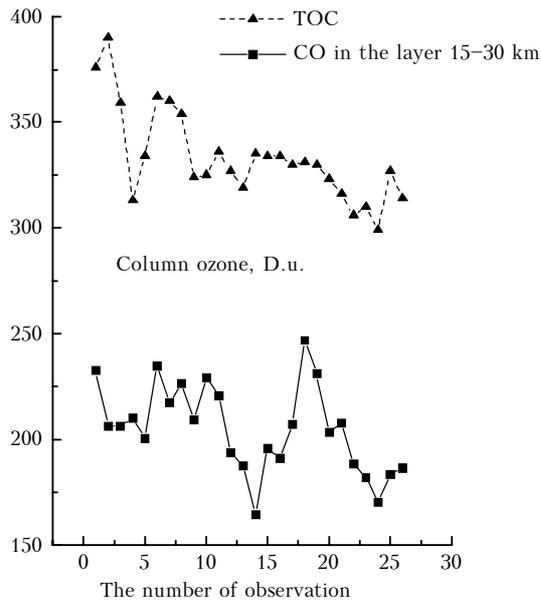
Fig. 7. Series of selected TOC values (M–124 device) and column ozone in the layer of 15 to 30 km (lidar) for the summer of 1998.

It seemed interesting to find the coefficient relating the lidar values of the integral column ozone in the layer of 15 to 30 km to the TOC values. This coefficient turned out to be $K = 0.616 \pm 0.056$, that is,

the mean column ozone in the 15 to 30 km layer for the summer period made up to 61.6 % of TOC. This value is somewhat lower than the mean content in this layer for mid-latitudes (about 65 %), which is given by Khrgian (Ref. 1). The discussed VOD measurements have been conducted simultaneously with measurements of vertical temperature distribution (VTD) by molecular scattering of radiation at the reference wavelength $\lambda_{off} = 353$ nm. The spatiotemporal resolution for VTD and the altitude range of VTD sounding were the same as for VOD. For the ozone and temperature profiles we have calculated the altitude behavior of the correlation coefficient presented in the Table 1.

It follows from the Table that the correlation between the ozone concentration and air temperature is positive in the altitude ranges of 17 to 26 and 28 to 30 km. This conclusion is in a good agreement with the data from Ref. 1. The statistically confident positive correlation between the ozone concentration and atmospheric temperature is most likely caused by the influence of the dynamic and radiation factors. In accordance with known ozonometric Normand – Dobson principle,[1] the dynamic factor manifests itself through vertical motion of air masses in the stratosphere: the downward motion is accompanied by accumulation of ozone and adiabatic heating of air, while the upward motion is accompanied by ozone consumption and adiabatic cooling of air.

Table 1. Coefficient of correlation between the temperature and ozone concentration K^* at altitudes from 15 to 30 km.

H, km	15	16	17	18	19	20	21	22	23	24	25.2	26.4	27.6	28.8	30
K^*	−0.36	−0.21	0.23	0.47	0.50	0.66	0.78	0.74	0.49	0.60	0.41	0.26	-0.31	0.15	0.22

In the stratospheric layers at the altitudes of 15 to 16 and 27 to 28 km, the correlation coefficient is negative. It is particularly remarkable that according to the literature data [12,13] and the data of our long-term observations, secondary maxima of column ozone are most probable just at these altitudes. It can be assumed that the lower secondary maximum is caused by a horizontal advection of northern air masses, while the upper one is caused by the meridional circulation of the atmosphere. Both cases involve transfer of ozone-rich air masses because air mass transfer occurs at the altitudes of polar and tropical maxima of ozone. In both of these cases, the temperature of air masses coming from north and south is below the temperature of mid-latitude air masses at these altitudes. For example, at the altitude of 27 to 28 km the air temperature in mid-latitudes in summer is 3–4 j higher than in the tropics.[14] From the above-said we can conclude that the cause of the observed negative correlation between the column ozone and temperature at altitudes of 15 to 16 and 27 to 28 km is the transfer of relatively cold air masses with high ozone content from north and south.

Acknowledgments

References

1. A.Kh. Khrgian, *Physics of the AtHosphere* (Gidrometeoizdat, Leningrad, 1969), 648 pp.
2. G. Megie et al., Nature, No. 270, 329 (1977).
3. O. Uchino, M. Maeda, and M. Hirono, JEEE J. Quant. Electr. **QE-15**, No. 10, 1094–1100 (1979).
4. M.P. McCormick, compiler, *Third International Lidar Researchers Directory*, NASA, Hampton, Virginia 23681–0001 (1993).
5. A.V. El'nikov, V.V. Zuev, V.N. Marichev, and S.I. Tsaregorodtsev, Atm. Opt. **2**, No. 9, 841–842 (1989).
6. V.V. Zuev, M.Yu. Kataev, and V.N. Marichev, Atmos. Oceanic Opt. **10**, No. 9, 691–698 (1997).
7. G.N. Glazov, *Statistical ProbleHs of Lidar Sounding of the AtHosphere* (Nauka, Novosibirsk, 1987), 312 pp.

8. V.G. Astafurov and A.A. Mitsel', Avtometriya, No. 1, 92–97 (1984).

9. A.J. Krueger and R.A. Minzher, J. Geophys. Res., No. 81, 4472 (1976).

10. V.V. Zuev, V.N. Marichev, and V.S. Smirnov, in: *Abstracts of Reports at the Fourth SyHposiuH on AtHospheric and Oceanic Optics*, Tomsk (1997), pp. 219–220.

11. V.N. Marichev, *ReHote Optical Sensing of Aerosol, TeHperature, and Minor Gaseous Constituents of the AtHosphere*, Doctor Phys.-Math. Sci. Dissert., Tomsk (1998), 270 pp.

12. *AtHosphere. Handbook* (Gidrometeoizdat, Leningrad, 1991), 510 pp.

13. V.E. Zuev and V.S. Komarov, *Statistical Models of TeHperature and Gaseous Constituents of the AtHosphere* (Gidrometeoizdat, Leningrad, 1986), 264 pp.

14. I.I. Ippolitov, V.S. Komarov, and A.A. Mitsel', in: *Spectroscopic Methods of AtHospheric Sounding* (Nauka, Novosibirsk, 1985), pp. 4–41.